Study on Shape Characterization of Crystalline Particles: Analysis of the Standard Deviation of the Angular Projection Function

J. A. Poce-Fatou, J. Martín,* and R. Alcántara

Departamento de Química Física, Facultad de Ciencias, Apartado de Correos 40, 11510 Puerto Real (Cádiz), Spain

Received: August 7, 2001; In Final Form: March 28, 2002

The analysis of the shadows projected by a particle on a plane may be used as a basis for a study of particle three-dimensional shape and size. In that study, a mathematical function describing the value of the area projected by a particle in every spatial orientation could be a very useful tool. In the present work, a method for calculating the angular projection function (apf) of a flat-sided convex solid has been developed. The standard deviation of the apf signal spectrum has been calculated for different model particles and found to be useful as a distinctive signature of particle shape. The relationship between this signature and the noise associated with the transmittance of a suspension has been discussed.

Introduction

Modeling is a very useful tool used in science to understand data. For example, it is used with light scattering devices to calculate the size distribution and absolute concentration of the particles suspended in a solution. In the case of spherical particles, the scattered intensity distribution allows us to calculate their size distribution. Furthermore, if intensity data of the unscattered beam is considered, the absolute concentration is obtained.[1] However, for a particle shape other than a sphere, the approximation is wrong. In these cases, a proper shape modeling is crucial for understanding experimental data.

The problem of particle characterization may be analyzed from projected area determination.[2] Therefore, the definition of mathematical functions describing the projected areas of nonspherical particles represents an effective tool for such characterization. In the interpretation of light scattering measurements, the information included in the cumulative distribution functions and, furthermore, in the probability density functions[3] has been proved to be useful as signatures for specific shapes.[4] From the analysis of these functions it is derived, for example, that in the prediction of nonspherical diffraction patterns it is not necessary to consider all possible orientations because some of them are more representative than others. In addition, by using maximum-likelihood estimators, particle size can be obtained.

A solution to the problem of calculating the probability distribution and density functions for circular cylinders and cuboids was found by Walters[5] and Vickers.[6] In this work we present an alternative method to obtain a function related to these, the angular projection function, for a flat-sided convex solid. To assist in the interpretation of the unscattered beam in light diffraction measurements and image analysis, we analyze the role of the standard deviation of its signal spectrum as a distinctive signature of shape.

Finally we focus attention on the theoretical relationship between this signature and the noise associated with the transmittance. The discussion is based on experimental data obtained with laser techniques for detecting growth nuclei in supersaturated solutions[7,8] and computerized simulation studies carried out on this subject.[9−11]

Materials and Methods

Shape Models. We want to analyze the possibility that the standard deviation of the signal spectrum of the areas projected by a nonspherical particle could be useful as a signature to discriminate shape. To that end, we will study a set of model shapes that can easily be described and analyzed from a mathematical point of view. The selection of these models and the terminology used are based on mathematical criteria.

As shown in Figure 1, the particles are prismatic with 3-, 4-, and 6-sided faces, known in this work as P3, P4, and P6, respectively. By adding two opposing pyramids to each one of these we obtain another set of three particles which will be known as P3P, P4P, and P6P. The bases of each one of these particles are regular polygons whose edge we will call *main edge*. P3, P4, and P6, have been analyzed in a whole variety of lengths ranging from $l = 0.25$ to $l = 3.00$ times the length (L) of the main edge. A special length of $l = 0.10$ has also been included to emulate a quasi-flat particle.

The opposing pyramids of prisms P3P and P4P are formed by equilateral triangles whose side lengths are equal to the main edge. However, this is not possible in the case of the 6-sided polyhedron, since the bases on which the 6-sided pyramids are placed are regular hexagons, and the only possible disposition of equilateral triangles on such bases would have to be on the same planes. In this case, the height of the pyramid has arbitrarily been assigned a value equal to the length of the main edge. P3P, P4P, and P6P have been analyzed within the same length range as P3, P4, and P6, although the study has been extended to include the special case $l = 0.00$, for which the particles P3P, P4P, and P6P become bipyramidal variants without prismatic structure. Finally, the values $l = 100.00$ and $l = 1000.00$ have been included, as parameters representative of very elongated structures.

The Angular Projection Function, $F(\theta, \phi)$. The angular projection function $F(\theta, \phi)$ takes the value of the area projected by a particle in every spatial orientation. To obtain it, we first

* Corresponding author. Phone: 34 956 016 332. Fax: 34 956 016 228. E-mail: joaquin.martin@uca.es

10.1021/jp0130618 CCC: $22.00
Published on Web 06/07/2002

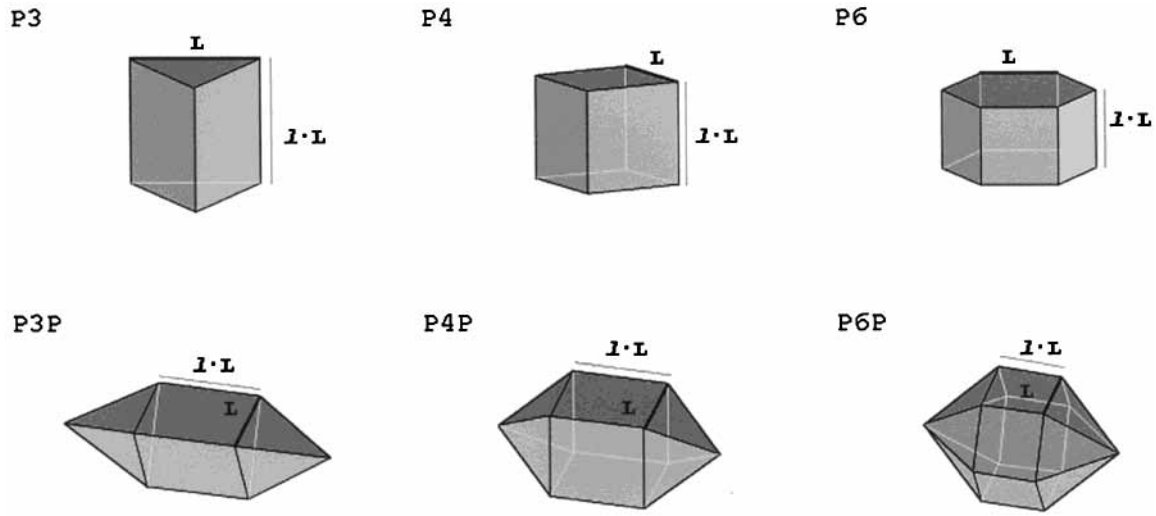

Figure 1. Description of shape models. Every particle shows a thicker line, which indicates the principal or main edge. A line has been drawn next to each particle, to show the edge that defines its length. This may be from 0.00 to 3.00 times (l) the length of the principal edge (L). In this figure, only 1.00 lengths have been drawn.

analyze a model consisting of one single freely rotating particle that projects its shadow onto a fixed plane. On the basis of this model, we describe an equivalent one, which has the advantage that it simplifies the analytical treatment required to calculate the angular projection function. In the latter model, the particle to be analyzed is placed at a fixed position, unable to rotate or move. The projection plane, which had a fixed position in the original model, can move and is at all times tangent to an enclosing sphere surrounding the particle. The direction of this moving plane coincides with that of its normal vector. Its Cartesian coordinates (x,y,z) can be expressed as a function of the spherical coordinates ρ, θ, and ϕ, from the following equalities:

$$x = \rho \sin(\theta) \sin(\phi)$$
$$y = \rho \sin(\theta) \cos(\phi)$$
$$z = \rho \cos(\theta) \quad (1)$$

If we use a unit radius sphere, i.e., where $\rho = 1$, the directions evaluated can simply be expressed as a function of the angular coordinates (θ,ϕ).

The particles evaluated in this study are flat-faced convex solids. Given that every face is represented by a normal vector, the surface projected by face i (A_i) onto the mobile plane is determined by the magnitude of the scalar product of their normal vectors. The area of every face is a distinctive feature of each shape, and therefore, all we have to do in order to calculate the projected surface is solve $\cos(\psi_i)$, where ψ_i is the angle formed by the normal vector to face i and the normal vector to the projection plane.

Figure 2 shows a front and back view of an octahedral particle, (P4P with $l = 0.00$), as seen from the direction perpendicular to the plane of the paper. In both cases, the projected surfaces coincide, and its area may be calculated from the contribution made to it by the faces observed in each case. If we consider the front view, the faces involved in the projection of the total surface are S1, S2, S3, and S4. If we consider the opposite view, the faces involved are S5, S6, S7, and S8. If, furthermore, we consider that the normal vector to the projection plane is directed toward the front view plane, we will have that the scalar product of this vector and the vectors representing faces S1, S2, S3, and S4 is positive. On the contrary, the scalar product of the normal vector to the projection plane and those representing faces S5, S6, S7, and S8, is negative. Regardless of the sign of the scalar product, the surfaces projected by the front or back faces coincide. Therefore, the angular projection function can be defined including all faces of the convex solid as

$$F(\theta, \phi) = \sum_{i=1}^{n} \frac{|A_i \cos(\Psi_i)|}{2} \quad (2)$$

where the projection of the particle in the direction given by (θ,ϕ), is calculated as half the summation of the surface area projected by each face. According to eq 2, the angular projection function is expressed in terms of the area of each face and the cosine of the angle between its normal vector and that of the orthogonal projection plane (scalar product).

We now describe the procedure to follow in order to calculate these functions: (1) We label the vertices of the particle fixed at any given spatial location and define their Cartesian coordinates. (2) The vectors forming every edge are calculated subtracting from them the coordinates of the adjacent vertices. (3) The coordinates of the normal vectors to each face are calculated as the vector product of the edge-vectors that meet at a vertex (we will take into account the corkscrew rule to define in every case the coordinates of the normal vector pointing to the outside of the volume). (4) The area A_i of every face will be given by the magnitude of the corresponding normal vector.

Following this procedure, the angular projection function is easily obtained. For example, for P4 it is given by

$$F_{P4}(\theta, \phi) = lL^2 (|\sin(\theta) \sin(\phi)| + |\sin(\theta) \cos(\phi)|) + L^2 |\cos(\theta)|; \quad (3)$$

Once it has been obtained, the standard deviation (SD) is calculated by

$$\mathrm{SD} = \sqrt{\overline{F^2}(\theta, \phi) - \overline{F}^2(\theta, \phi)}; \quad (4)$$

The second term of the square root can easily be solved by Cauchy's theorem,[12] which states that the average geometrical projected area of a convex particle with random orientation is

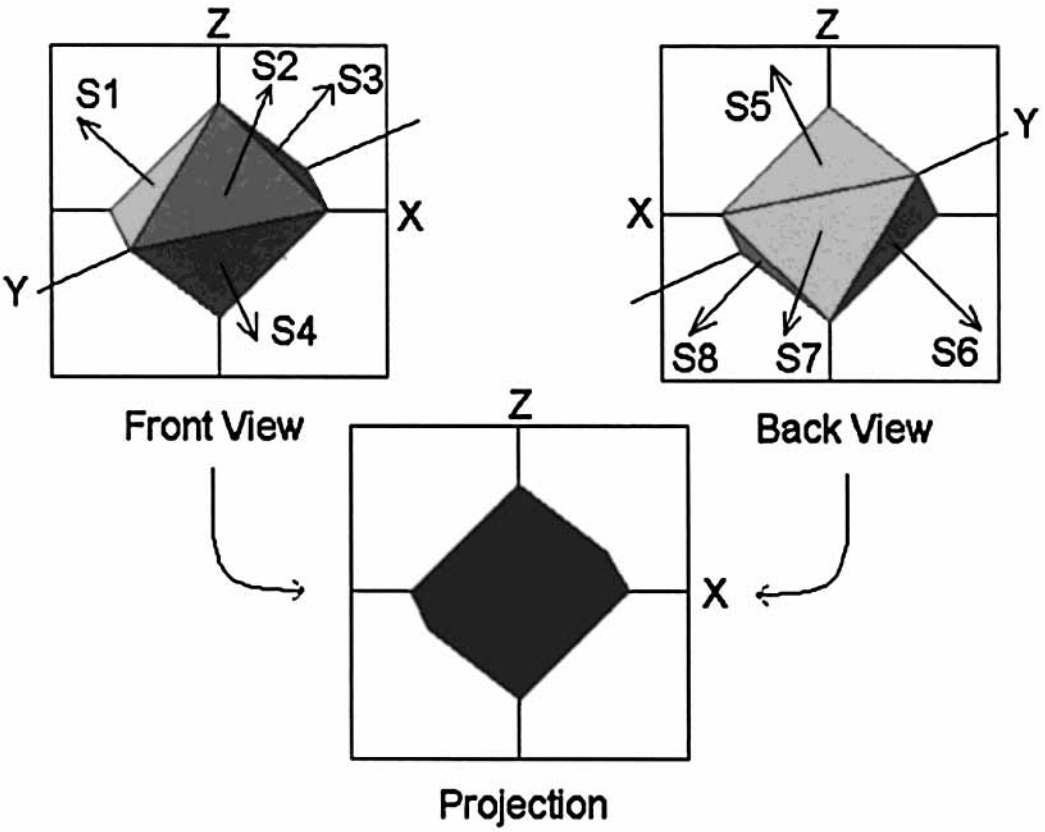

Figure 2. An octahedral particle (P4P with $l = 0.00$) observed from points of view diametrically opposed to each other. In both cases the surface projected onto a fixed plane perpendicular to the axis of observation coincide.

one-quarter of the total surface area (S),

$$\bar{F}(\theta, \phi) = \frac{S}{4} \tag{5}$$

The first term can be calculated by

$$\overline{F^2}(\theta, \phi) = \frac{2\int_0^{2\pi}\int_0^{\pi/2}\sin(\theta)F^2(\theta, \phi)\,d\theta\,d\phi}{2\int_0^{2\pi}\int_0^{\pi/2}\sin(\theta)\,d\theta\,d\phi} \tag{6}$$

where $\sin(\theta)$ represents the functional or Jacobian determinant for the mapping transformation of Cartesian coordinates into spherical coordinates. Knowing the minimum and the maximum value of the projected area, this term or indeed the mean of some higher power can alternatively be calculated by using the cumulative distribution function of the projected area or the probability density function.[5,6]

Comparable Volumes. There is clearly a relationship between the projected areas SD and the size of the particle. The larger the volume, the larger the projected areas and the higher the absolute values of the variations caused by changes in the orientation. For this reason, to establish a relative comparison among different shapes, it is convenient to set a criterion that eliminates the influence of size.

Let us compare the model used to calculate the $F(\theta, \phi)$ functions to an ideal sample consisting of one single isolated particle suspended in a solution. Let us suppose that a laser beam whose section is much larger than the particle's is crossing this sample, and let us examine the amount of unscattered light. The particle changes randomly its orientation and its position, keeping inside the beam volume and projecting its orthogonal image on a fixed plane. As the fraction of light obscured by the particle is related, by the Beer−Lambert law, to the transmittance, we establish the criterion of comparing those particles that would generate similar levels of transmittance, i.e., same values of $\bar{F}(\theta, \phi)$.

Results and Discussion

Selecting an average projection area, $\bar{F}(\theta, \phi)$, of 100 units, the SD of the $F(\theta, \phi)$ signal spectrum was calculated and plotted against the length factor (l) in Figure 3. P3, P4, and P6 show maximum values of noise for small values of l. For $l = 0.10$, the particle with the highest level of noise is P6, followed by P4, and finally P3. Therefore, for small values of l (semi-flat particles), the higher the number of faces of the polyhedron, the higher will be the level of the SD. In theoretical terms it seems obvious that when l tends to zero, the SD tends to infinity. This trend tends to reverse as the length parameter increases. It can be seen that for $l = 3.00$, the shape with a higher level of SD is P3, followed by P4, and, finally P6. It is worth pointing out that each one of these three particles shows a minimum on the curves in Figure 3.

The plots of the curves of P3P, P4P, and P6P are distinctively different from the former ones. In this case, the variations observed in the SD, in the $l = 0.00$ to $l = 3.00$ range, are not so sharp. The behavior of P3P shows there is no minimum. P4P shows a barely perceptible minimum at $l = 0.10$, whereas in the case of P6P there is a clear minimum at $l = 0.50$. As the relative length of all the particles analyzed increases, the difference between the SDs tends to minimize. In the hypothetical limit in which the particles are long needlelike shapes, so that they are barely distinguishable one from the other (l tends to infinity), the SD must be very similar. The closeness of the values obtained for the SD when $l = 100.00$ and $l = 1000.00$ confirms this argument.

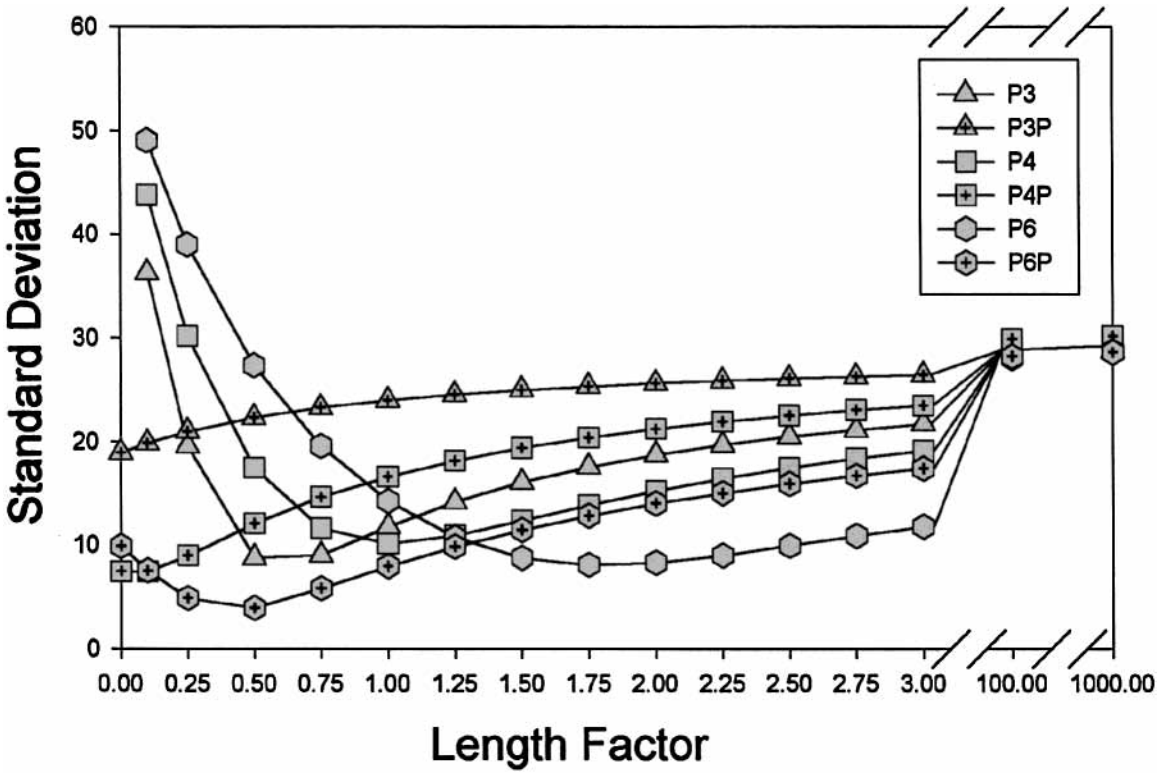

Figure 3. Shape classification in terms of the standard deviation.

Standard Deviation as a Measure of the Noise Associated with the Transmittance. The uncertainty inherent in every experimental measurement can be caused by the performance of the instrumentation, imperfections of the experimental design, changes undergone by the physical chemical parameters of the system, etc. In this context, we use the term "noise" to refer to all the deviations detected between the exact and experimental values.

In the ideal one-particle system crossed by a laser beam described above, as long as the particle remains in the beam volume, the only cause of variation in the transmittance are the changes in the orientation of the particle. In these conditions, the SD of $F(\theta, \phi)$ signal spectrum becomes a measure of the level of noise associated with the transmittance.

However, in actual experiments there is not just one single particle but many of them. In these systems, the noise associated with the transmittance may be derived from two additional sources, one being the different sizes that particles may have and the other being the particles' interference with each other. We have recently analyzed experimental systems in which crystalline precipitates were generated.[8] By using solutions within a wide range of concentrations, it was observed that practically flat particles ($l \approx 0$) generated high levels of noise in relation to the noise generated by elongated particles. In those experiments the laser beam was focused, which added a further source of noise, caused this time by the different positions at which particles could be intercepted by the beam.

The computational simulation of these experiments was also carried out. Under the same virtual conditions, particles systems with different shapes generated different levels of noise.[11] According to these data and according to the model analyzed in this work, it seems that the higher levels of noise associated with the transmittance constitute a proof of the qualitative relationship between the shape of and the noise caused by crystalline particles.

Indeed the problem of deducing the actual sizes and shapes of particles from just the associated noise is clearly impossible, so that the analysis of this signal should be considered here to be a useful source of information for understanding data. It is clear that a deeper study on this relationship should be carried out in order to elucidate the conditions for which the source of noise caused by the shape of particles arises from others.

Conclusions

A method for calculating the angular projection function of flat-sided convex particles is presented. Although it has been applied to a set of model shapes, it may be used for the study of any crystallographic model. The SD of this function's signal spectrum is an interesting discriminator of shape, which could be used as a help in the interpretation of the transmittance signal in laser light diffraction measurements and image analysis. Both the theoretical studies carried out in this work and the experimental data of previous studies allow us to state that the noise associated with the transmittance of a system consisting of crystalline particles suspended in a solution is related to the shapes of such particles.

Acknowledgment. This work was funded by the Spanish CICYT under Grant ALI97-0885.

References and Notes

(1) Brown, D. J.; Felton, P. G. *Chem. Eng. Res. Des.* **1985**, *63*, 125−132.
(2) Umhauer, H.; Gutsch, A. *Part. Part. Syst. Charact.* **1997**, *14*, 105−115.
(3) Vickers, G. T.; Brown, D. J. *Proc. R. Soc. London A* **2001**, *457*, 283−306.
(4) Brown, D. J.; Vickers, G. T. *Powder Technol.* **1998**, *98*, 250−257.
(5) Walters, A. G. *Proc. Camb. Philos. Soc*. **1947**, *43*, 343−347.
(6) Vickers G. T. *Powder Technol.* **1996**, *86*, 195−200.

(7) Martín, J.; Alcántara, R.; García-Ruiz, J. M. *Cryst. Res. Technol*. **1991**, *26*, 35−42.

(8) Poce-Fatou, J. A.; Alcántara, R.; Gallardo, J. J.; Martín, J. *Comput. Chem.* **2001**, *25*, 447−457.

(9) Poce-Fatou, J. A.; Alcántara, R.; Martín, J. *Comput. Chem.* **2001**, *26/2*, 131−140.

(10) Martín, J.; García-Ruiz, J. M.; Alcántara, R. *Cryst. Res. Technol.* **1992**, *27*, 799−808.

(11) Poce-Fatou, J. A., Ph.D. Thesis, Universidad de Cádiz, 1999.

(12) Cauchy A. *Oeuvres Complètes d'Augustin Cauchy*, 1re série, Tome II.; Gauthier-Villars: Paris, 1908.